Prototype 250 GHz Bandwidth Chip to Chip Electrical Interconnect, Characterized With Ultrafast Optoelectronics

Jeong Sang Jo, Tae-In Jeon, and Daniel R. Grischkowsky, *Fellow, IEEE*

***Abstract*—We have connected two optoelectronic chips with air-spaced two-wire transmission lines and have observed essentially undistorted transmission of 1.8 ps (FWHM) electrical pulses over propagation distances up to 200 cm. The lines consist of two 0.4 mm (or 0.5 mm) diameter copper wires with centers separated by 1.0 mm. The air spaced two-wire lines show transform-limited TEM mode pulse propagation with very small group velocity dispersion (GVD), and relatively low attenuation. Our achieved performance with a power loss of 5.8 dB/m approaches that needed for mm-wave and THz interconnects. The coupling was enabled by two tungsten probes with 1 μm diameter tips in near-contact (5 μm gap) with the coplanar transmission lines on the transmitting and receiving optoelectronic chips. The air spaced two-wire line's relatively small, measured pulse amplitude attenuation coefficient was 1.31 times larger than the theoretical prediction for the TEM mode. This discrepancy is considered to be primarily due to reduction of the Cu conductivity in the THz skin-depth layer.**

***Index Terms*—Terahertz (THz), two-wire, pulse propagation, amplitude attenuation, low-loss.**

I. Introduction

AT PRESENT, no electrical interconnect is available to transmit undistorted ps electrical pulses for distances of several meters with acceptable loss. Commercially available high-bandwidth coaxial cable is specified to have a power loss of 260 dB/100 ft (equivalent to 8.5 dB/m) at 50 GHz.[1] This loss is mainly due to the PTFE (Teflon) dielectric, and for the same radial geometry of the commercial cable, the loss increases linearly with frequency to a loss of 85 dB/m at 500 GHz. This power loss has been previously measured to be 278 dB/m at 500 GHz for a much smaller radial geometry coaxial cable [1]. Consequently, the lack of this key component prevents many technical applications and stimulates the search for such an interconnect.

The lack of a high-bandwidth electrical chip to chip interconnect has led to optically interconnected electronic chips and devices [2]–[4]. However, the optical-link requires non-silicon devices to generate and modulate optical signals and then coupling to optical fibers and waveguides, resulting in increased complexity and cost. The ultimate example of the optical interconnect is that for the highest speed supercomputers, which are connected together by thousands of single mode optical fibers with bit rates of up to 50 Gb/s. For this case, the output electrical signal (bit) is converted to a light pulse coupled into the fiber, and at the output end of the fiber at the attached computer, the light pulse is then converted back to the electrical signal [5].

The experimental demonstration and characterization of the chip to chip electrical interconnects described in this paper, show essentially undistorted transform limited propagation of a 1.8 ps pulse up to a distance of 2000 mm for our latest Type-II, two-wire transmission line with the comparatively-low[1] power loss of 5.8 dB/m within the frequency range from 50 to 300 GHz. These results present a possible solution to the high-bandwidth electrical interconnect problem.

Using two matched electrical probes we have efficiently connected two optoelectronic chips with air-spaced two-wire transmission lines. The pulses were generated by photo-conductively switching a charged coplanar transmission line on the optoelectronic transmitter (Tx) chip [6]–[8]. These pulses were then efficiently coupled to the two-wire transmission line by two matched probes. After propagation over the two-wire line, the pulses were again efficiently transferred to the coplanar transmission line of the receiver (Rx) chip, via near-contact coupling with two probes, one for each wire. The coupled pulses were then optoelectronically measured on the Rx chip.

Many different waveguides and transmission lines have been tested for guiding of mm and THz electromagnetic waves, such as metal tubes [9], parallel plates [10], coaxial cables [1], two-metal wires [11]–[17], and single metal wires [18], [19]. In order to use any of these waveguides for an application, single-mode propagation is usually required. For digital applications TEM-mode propagation is required, because of no cutoff frequency, and consequently no waveguide-mode group-velocity dispersion (GVD). Among various types of THz waveguides, the two-wire line is ideal in terms of the excellent coupling to the coplanar transmission line on our

Manuscript received December 11, 2012; revised February 23, 2013; accepted March 01, 2013. Date of publication April 05, 2013; date of current version June 27, 2013. This work was supported in part by the National Research Foundation of Korea (NRF) and the Korea Science and Engineering Foundation (KOSEF) grant funded by the Korea government (MEST) under 2010-0009070 and 2008-0062257, and in part by the U.S. National Science Foundation (NSF) under Grant 0757680.

J. S. Jo was with the Division of Electrical and Electronics Engineering, Korea Maritime University, Busan, 606-791, South Korea. He is now with the Center for Quantum-Beam-based Radiation Research, Korea Atomic Energy Research Institute, Daejeon, 305-353, Korea.

T.-I. Jeon is with the Division of Electrical and Electronics Engineering, Korea Maritime University, Busan, 606-791, South Korea (e-mail: jeon@hhu.ac.kr).

D. Grischkowsky is with the School of Electrical and Computer Engineering, Oklahoma State University, Stillwater, OK 74078 USA (e-mail: daniel.grischkowsky@okstate.edu).

Digital Object Identifier 10.1109/TTHZ.2013.2251930

[1]Pasternack Enterprises, Inc., Irvine, CA 92623 USA. [Online] Available: www.pasternack.com

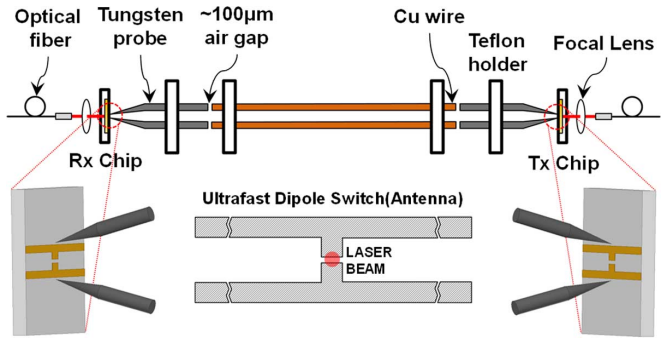

Fig. 1. Experimental setup.

Tx and Rx chips; in addition, the THz beam propagates in air, thereby eliminating dielectric loss, and is well guided by the TEM mode propagation on the two metal wires. The remaining practical problem is how to support the wires and how to maintain their separation without disturbing the TEM mode propagation [11]–[17]. A significant step to realize this is the work on coplanar transmission lines on low-permittivity substrates [13].

II. Experimental Setup

Commercial copper (Cu) wires of 0.4 mm (or 0.5 mm) diameter and various lengths are used for the measurement. The two-wire transmission line with 1.0 mm separation between the wire centers is supported and put under tension by two or three tightly fitting 25 mm diam. Teflon holders of 3 mm thickness at the ends of the line, similar to those used in the previous report [19].

The photo-excitation of the biased dipole switch (antenna) imbedded in the coplanar transmission line as shown in Fig. 1, generates two counter-propagating electrical pulses down the line and excites a short burst of radiation due to the photocurrent pulse, which has the shape of the derivative of the current pulse. We couple to the current pulse with the probes. It is best to make contact near the dipole switch or on the switch in order to couple out the shortest electrical pulse, which rapidly broadens with propagation down the coplanar line [6], [8].

Two 30-mm-long commercial tungsten (W) probes are used to make the coupling between the THz pulses and the Cu wires. The probes consist of a 0.5 mm diameter W cylinder for 25 mm that terminates in a 5 mm long conical taper ending on the 1-μm diameter probe tip. The 25-mm-long cylindrical ends of the probes are supported by the same type of tightly fitting Teflon holders used for the Cu wires. As shown in Fig. 1, the two 1-μm tips are near-contact (with 5 μm gap) to the dipole switch on the silicon on sapphire (SOS) Tx or Rx chips. The cylindrical end faces of the probes and end faces of the Cu wires are closely spaced with air gaps of about 100 μm. The observed signal strength is only increased by 3% with a 25 μm gap and drops by 2% if the gap is increased to 150 μm [20]. Direct contact would only increase the signal by 4%, but would disturb and possibly damage the delicate connection at the tapered end. Consequently, the W-probe tips and the dipole antenna chips are rigidly fixed. Thereby, the THz wave coupling to the W-probe tip remains the same, when the air-spaced two-wire lines are replaced by air-spaced two-wire lines of different lengths.

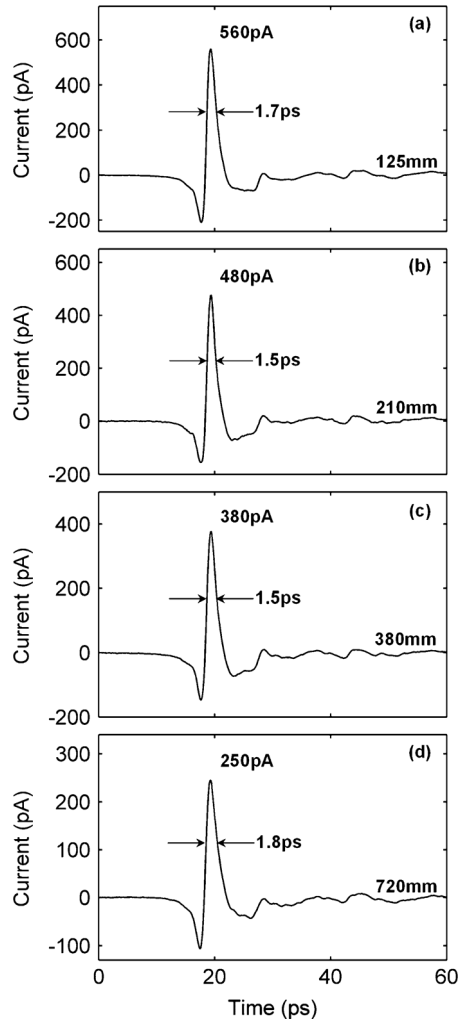

Fig. 2. (a)–(d) Measured THz pulses for the Type-I air spaced two-wire lines lengths of 125, 210, 380, and 720 mm, respectively.

A Ti-sapphire mode-locked laser provides 41 and 28 mW of average power to the generation and sampling beams of the 0.18 ps, 780 nm pulses at a repetition rate of 83 MHz from the two optical fibers guiding the laser beams to the Tx and Rx chips. The fiber guided laser beams are focused on the 5 μm gaps of the photoconductive dipole switches, situated between the two 10 μm lines separated by 30 μm of the coplanar lines on the optoelectronic chips, as shown in Fig. 1. The coplanar lines extend for 10 mm on each side of the dipole switch in order to eliminate short delay time reflections.

III. Measurement and Analysis

The measured THz pulses, transmitted over our initial Type-I, 125-mm, 210-mm, 380-mm, and 720-mm-long air spaced two-wire lines (400 μm dia. 1 mm, center to center separation) with two Teflon holders are displayed in Fig. 2. The THz pulses shown in Fig. 2(a)–(d) are remarkably similar to each other in complete detail, indicating the negligible GVD expected for the TEM mode propagation. The peak amplitudes of the reference THz pulses are reduced only 55% by extending the wire

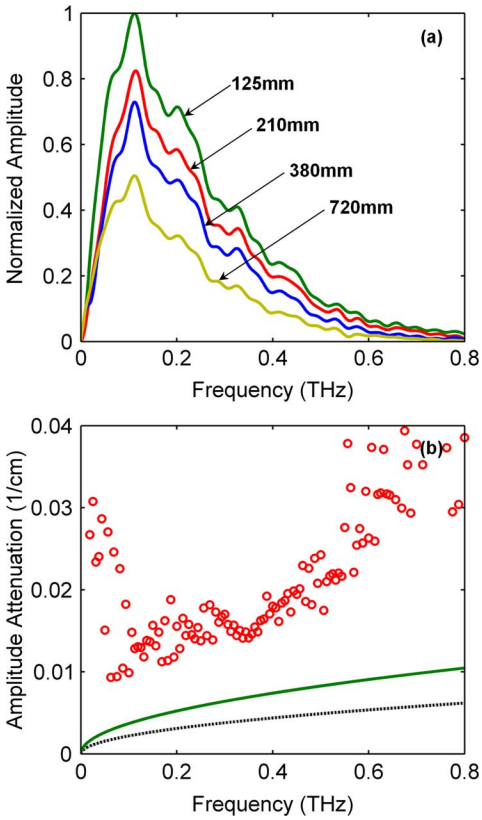

Fig. 3. (a). Corresponding amplitude spectra of the THz pulses shown in Figs. 2(a)–(d). (b). Measured amplitude attenuation coefficients of the Type-I air spaced two-wire lines (open circles), and the calculated absorption coefficients for the air spaced two-wire lines (solid top line), and a Cu PPWG with a 1.0 mm gap (dashed bottom line) for Cu conductivity of 5.8×10^7 (Mhos/m). For units conversion, an amplitude attenuation of 0.01 /cm corresponds to a power attenuation of 0.02 /cm, which is equivalent to a power attenuation of 8.7 dB/m.

from 125 to 720 mm. The amplitude attenuation with propagation distance is simply described by $\exp[-\alpha \mathrm{L}]$, for which $\alpha = 0.014$/cm. This result predicts a pulse height of $560 \times \exp[-2.8] = 34$ pA for a propagation distance of 2000 mm. This 34 pA signal could be easily measured with our system with a noise level ± 0.8 pA. The relatively short pulse widths and small pulse attenuation in Fig. 2 show much less attenuation and broadening per unit length than previous optoelectronic pulse measurements on high bandwidth solid copper clad coaxial cables [1].

The corresponding THz pulse amplitude spectra are shown in Fig. 3(a), in which the spectrum bandwidth can be seen to extend up to 0.5 THz. Theoretically, for TEM mode propagation the amplitude absorption is expected to be very small for the air spaced two-wire lines, with an amplitude absorption coefficient of $\alpha(\omega) = 0.005$/cm at 0.2 THz [1], [21]. The corresponding power absorption coefficient of 0.01/cm is equivalent to power absorption of 4.3 dB/m. The theoretical TEM value of 0.005/cm is significantly smaller than the above measured value of $\alpha = 0.014$/cm from Fig. 3(b), describing the observed pulse attenuation. This extra-loss of THz propagating waves on metal has also been seen in parallel plate waveguide measurements [22], [23] and Zenneck THz surface wave measurements [24],

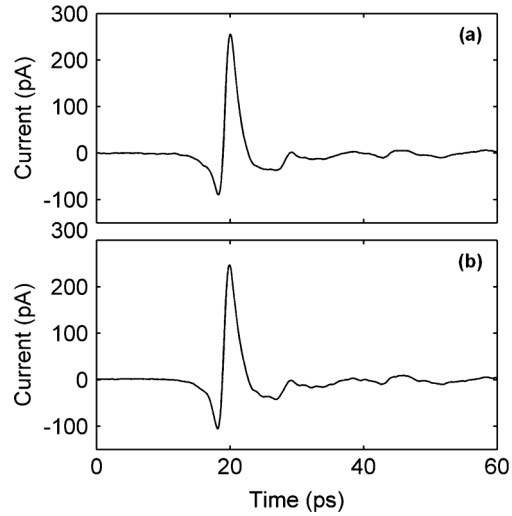

Fig. 4. (a) Calculated coherent THz output pulse, assuming an in phase frequency spectrum given by the measured 720 mm amplitude spectrum shown in Fig. 3(a). (b) Measured THz output pulse shown in Fig. 2(d).

[25], where it was explained by a reduction of the metal conductivity in the thin THz skin depth layer. The reduction in THz conductivity has also been observed in thin metal films [26]. For the two-wire line case of Fig. 3(b), this explanation would require a large reduction in conductivity by 4 times, in the skin depth region. Another possibility is co-propagating leaky mode radiation loss [27], [28]. This problem becomes important for $1 \leq \mathrm{d}/\lambda$, where d is the center to center separation of the wires and λ is the free space wavelength. For our high frequency limit 0.4 THz, $d/\lambda = 1.33$ and some leaky mode excitation may occur, but for the low frequency of 0.1 THz, $d/\lambda = 0.33$ and leaky-mode effects should be negligible. It is also important to note that the analytic TEM result is for a perfect two-wire line with no irregularities in wire diameters or spacing. In contrast, for the Type-I lines the spacing varies adiabatically [23] over the length of the line with the estimated spacing precision is 1.0 mm $\pm$ 0.3 mm. More abrupt variations can lead to significant scattering (radiation) loss.

The analytic solutions for amplitude absorption coefficients for the TEM propagation mode of the two-wire transmission line, the coaxial waveguide and the parallel plate waveguide (PPWG) are given in [1], [21]. For the Type-I air-spaced two-wire lines geometry with Cu wire diameters of 0.4 mm and center to center separation of 1.0 mm, the theoretical TEM amplitude absorption coefficient is 1.69 times larger than that for an air-spaced Cu PPWG with a plate separation of 1.0 mm, as shown in Fig. 3(b). The comparative absorption strength for an air-spaced coaxial waveguide with an inner conductor diameter of 0.4 mm and the inside radius of 1.0 mm to the outer conductor is 1.86 times larger than that for the PPWG. For these three waveguides the theoretical absorption is proportional to the square root of the frequency and inversely proportional to the square root of the conductivity.

The amplitude attenuation coefficients, calculated from the THz pulse spectra shown in Fig. 3(a) are obtained according to

$$\alpha_T = -\frac{1}{\mathrm{L}} \ln\left(\frac{A(\omega)}{A_0(\omega)}\right) \tag{1}$$

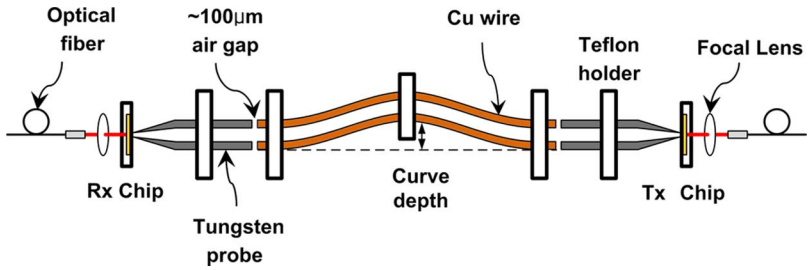

Fig. 5. Experimental setup to measure guiding strength as a function of curve depth for the Type-I two-wire line. The length of the two-wire line between the end Teflon holders is 170 mm. The actual curve depth was perpendicular to the ribbon geometry of the line to more easily maintain the 1 mm separation.

where $A(\omega)$ and $A_o(\omega)$ are the amplitude spectra transmitted through different lengths of the air spaced two-wire lines, and L is the effective wire length.

The measured amplitude attenuation for the air spaced two-wire lines shown in Fig. 3(b) is obtained by (1), for which $A_o(\omega)$ and $A(\omega)$ are the amplitude spectra of the 125-mm long (L_1) and 380-mm long (L_2) wires, respectively; $L = (L_2–L_1)$. The obtained attenuation is approximately 2.5 times larger than the theoretical calculation for the TEM mode.

Although the observed general trend is that the attenuation increases with frequency, in the region from 0.1 to 0.4 THz containing most of the pulse energy, the amplitude attenuation is reasonably constant about the value of 0.015/cm, corresponding to power attenuation of 0.03/cm, equivalent power attenuation of 13 dB/m. This feature explains the attenuation without reshaping pulse propagation results of Fig. 2.

In order to show the phase coherence of the 720 mm output pulse, the inverse fast Fourier transform (IFFT) was performed on the amplitude (magnitude) spectrum (which assumes all of the frequency components are in phase) and is shown in Fig. 4(a), in comparison to the observed pulse shown in Fig. 4(b). The similarity of this comparison shows the phase coherence of the output pulse and the importance of this low dispersion, low GVD line for digital communications.

In addition to the attenuation and GVD of the two-wire line, it is important to measure the guiding strength with respect to curvature. Here, it will be shown that the two-wire propagating THz pulse is much more tightly bound than the single wire THz pulse, propagating as the THz Sommerfeld wave [19]. For the measurement setup shown in Fig. 5, consider that the two wires form a thin ribbon with a width equal to the wire separation, similar to a highway or a railroad track. The measured curvature is in the direction perpendicular to the plane of the ribbon, similar to rolling up the ribbon on a spool.

As shown in Figs. 6 and 7(a), the signal pulse and spectrum are relatively unchanged with a modest 0.8 cm curve depth smoothly changing over the 170-mm line. However, as the curve depth increases, notable changes occur in both the signal strength and the corresponding spectra, which show much larger reductions of the higher frequencies. It is expected that the curvature losses would be less with smaller separation between the wires and smaller d/a ratios. The measured loss of the two-wire line is directly compared to a previous measurement of curvature loss of the single wire THz Sommerfeld wave [19] in Fig. 7(b). Clearly, and as expected, the binding of the waves to the wires is much stronger for the TEM propagation

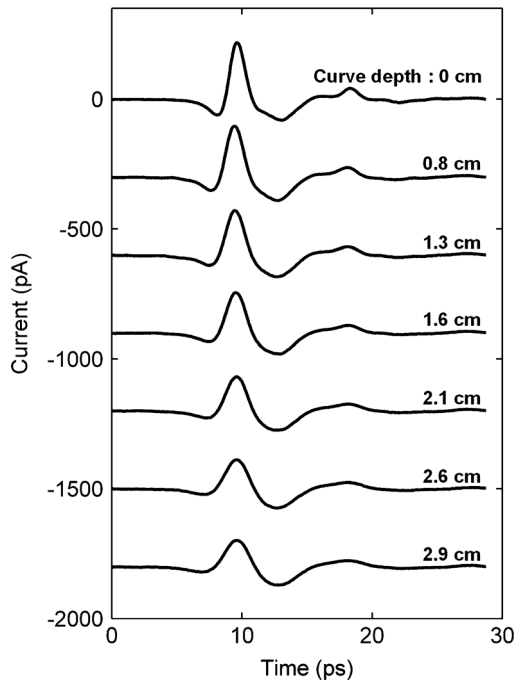

Fig. 6. Transmitted signal strength over the 170 mm long Type-I two-wire line with the indicated curve depths.

of the two-wire line. It is to be noted that the TEM mode of the two-wire line also applies to perfect electrical conductor (PEC) lines, while the Sommerfeld wave vanishes for a PEC line. Consequently, it is expected the measured binding strength of the TEM mode would be the same for perfect conductors.

Stimulated by the above set of Type-I measurements and their analysis, we have very recently performed another series of longer measurements with improved Type-II two-wire lines of 0.5 mm diameter with centers separated by 1.0 mm and lengths of 210, 1000, and 2000 mm, respectively. These Type-II wires match the diameter of the back face of the tungsten probes and give excellent coupling from probe to wire. The Type-II lines were constructed with three, much tighter and stronger Teflon holders, which hold the Type-II two-wire lines more precisely and with more tension. Consequently, the lines were straighter and with a more constant separation for the entire line. The precision of the separation for the Type-II is $1.0\ \mathrm{mm} \pm 0.2$ mm, and varies more slowly (adiabatically) [23] than for the Type-I line. Abrupt variations, which can lead to significant scattering (radiation) loss, are believed to be responsible for the significantly higher absorption of the Type-I line compared Type-II line.

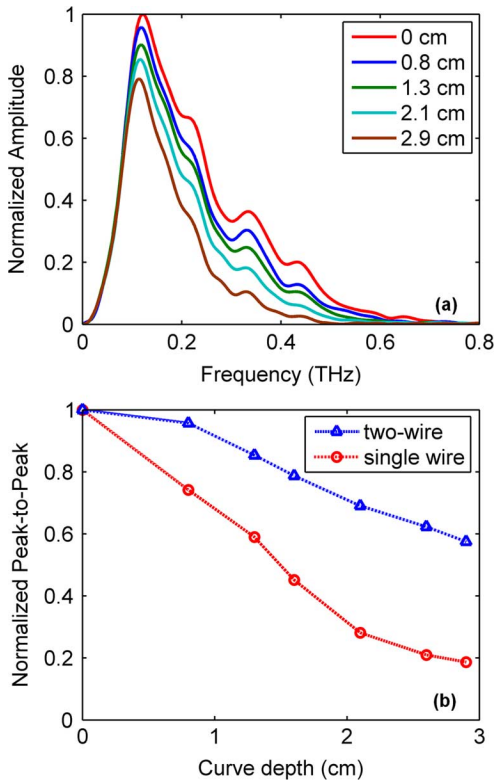

Fig. 7. (a) Corresponding amplitude spectra for the pulses shown in Fig. 6. (b) Normalized amplitude pulse peaks in Fig. 6 for different curve depths (top curve), compared to a similar measurement for single wire guiding (bottom curve).

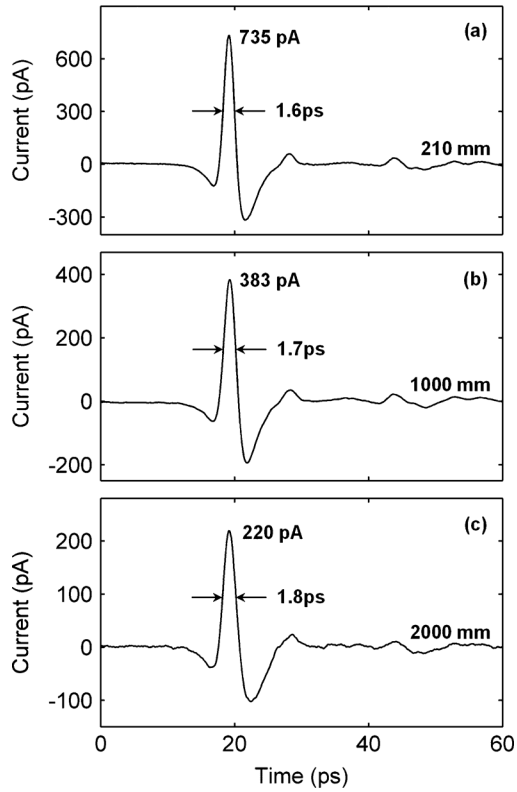

Fig. 8. Measured THz pulses (a)–(c) for the improved Type-II air spaced two-wire lengths of 210, 1000, and 2000 mm.

As shown in Fig. 8, these lines propagated transform limited pulses, resulting in a 1.6 ps FWHM pulse after 210 mm of propagation, a 1.7 ps pulse after 1000 mm, and a 1.8 ps pulse after 2000 mm with an amplitude S/N of 360:1. The slight broadening seen with propagation is due to attenuation of the higher-frequency components. The corresponding amplitude spectra for the pulses of Fig. 8 are shown in Fig. 9(a).

The amplitude attenuation coefficient α, obtained from the amplitude ratio (220/735) of the 2000-mm pulse to the 210-mm pulse, is $\alpha = 0.0067$/cm, compared to the theoretical value of 0.0051/cm at 0.2 THz, as shown in Fig. 9(b). The corresponding ratio of 1.31 for experiment attenuation compared to TEM theory can be reasonably explained by the expected reduction in THz conductivity in the skin depth [22]–[26]. The ohmic attenuation coefficient α increases as the conductivity σ decreases, where α is proportional to $1/(\sigma)^{1/2}$. Consequently an increase in attenuation by 1.31 would correspond to a decrease in conductivity by the factor of 0.58, within the range of the expected reduced conductivity.

The frequency-dependent amplitude attenuation for the 2000 mm measurement with respect to the 210 mm is shown in Fig. 9(b). The measured attenuation was calculated with (1), using $A_{\rm o}(\omega)$ and $A(\omega)$ for the 210- and 2000-mm-long wires, respectively. The attenuation measurement of Fig. 3(b) is also shown, together with the calculated absorption from two-wire TEM theory and the PPWG. The theoretical TEM amplitude absorption coefficient of the Type-II with 0.5 mm diameter and 1.0 mm center to center separation is 1.67 times larger than that for an air-spaced Cu PPWG with a plate separation of 1.0 mm.

Clearly, the Type-II, two-wire lines show enhanced measured performance compared to the Type-I lines. The measured amplitude attenuation for the 2000 mm Type-II, two wire line is consistent with an underlying square root frequency dependence with the Cu conductivity reduced by the factor 0.6. Below 140 GHz, the attenuation is reduced at 100 GHz, but goes to a relatively constant value at 50 GHz, the low frequency limit of our measurements. The cause of this extra low frequency attenuation is not known.

In order to show the phase coherence of the 2000 mm output pulse, the IFFT was performed on the amplitude (magnitude) spectrum and is shown in Fig. 10(a), In comparison to the observed pulse shown in Fig. 10(b). The similarity of this comparison shows the phase coherence of the output pulse and the importance of this low dispersion, low GVD line for digital communications.

In order to increase the depth of our understanding of the measurements made on the Type-II two-wire transmission line, an FDTD CST Microwave Studio numerical simulation was made for single frequency propagation with the results shown in Fig. 11. The wire waveguide was modeled in three dimensions which were bounded by a 3 mm (width) $\times$ 3 mm (height) $\times$ 10 mm (length) rectangular domain, with the two wire line located in the center. Approximately 5 million meshes, requiring typically 6 hours of running time, were used for each simulation to achieve accurate results, and the calculation loop was running until the ratio of old and new calculation results converged

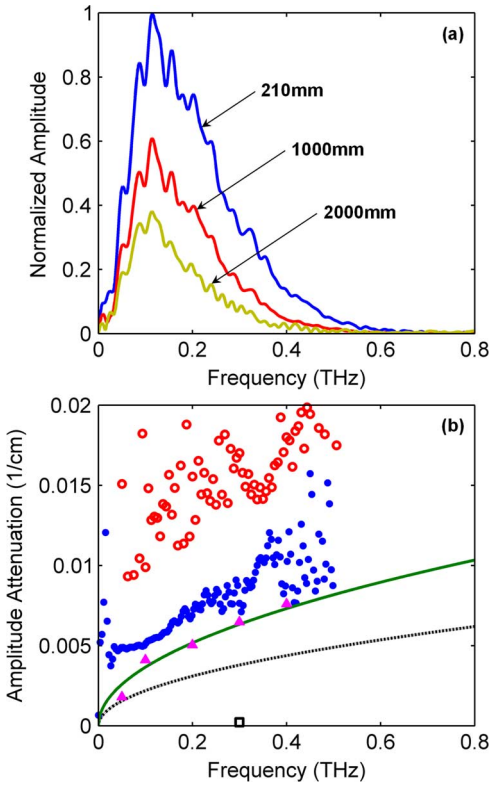

Fig. 9. (a) Corresponding amplitude spectra of the THz pulses shown in Figs. 8(a)–(c). (b). The attenuation of the Type-II two-wire line from the amplitude spectra of Fig. 9(a) is shown by the small dots. The larger attenuation of the Type-I two-wire line of Fig. 3(b) is shown by the open circles, together with the calculated absorption of the Cu two-wire TEM mode theory (solid upper line) and the TEM absorption of the PPWG (dashed lower line) as shown in Fig. 3(b) for Cu conductivity of 5.8×10^7 (Mhos/m). The pink triangles on the two-wire TEM theory curve mark the attenuation obtained from the simulation for 50, 100, 200, 300, and 400 GHz, respectively. The open square at 0.0002/cm for 300 GHz is the simulation attenuation for a perfect electrical conductor (PEC). The CST simulation will be described in detail below.

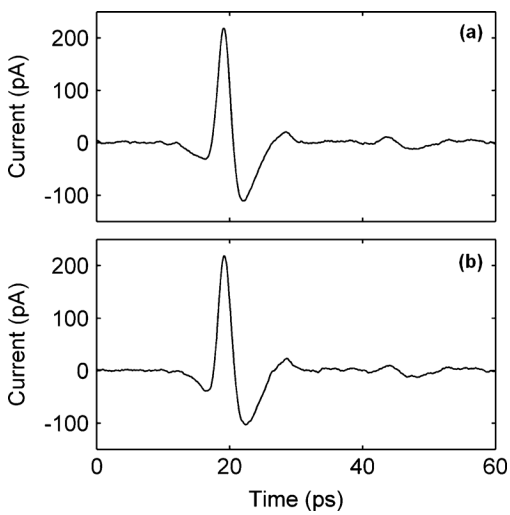

Fig. 10. (a) Calculated coherent THz output pulse, assuming an in phase frequency spectrum given by the measured 2000 mm amplitude spectrum shown in Fig. 9(a). (b) Measured THz output pulse shown in Fig. 8(c).

less than -50 dB. The copper wire is considered to have a conductivity of 5.8×10^7 (Mhos/m) or PEC. In this simulation, the

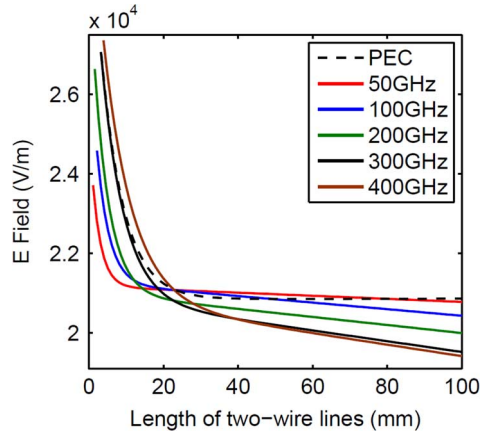

Fig. 11. FDTD CST numerical simulation of propagation 50, 100, 200, 300, and 400 GHz waves on Type-II two-wire Cu transmission line with wire diameters of 0.50 mm and center to center separation of 1.0 mm, and Cu conductivity of 5.8×10^7 (Mhos/m). The dashed black line indicates the simulation at 300 GHz for a perfect electrical conductor (PEC) line. The calculated vertical electric field strength at the mid-point between the two wires is shown.

plane wave is excited on the square input face of the rectangular tube. The outer wall of the domain is assumed to be an absorbing boundary to minimize any back reflections on the wires.

As shown in Fig. 11, after the input coupling of the single frequency THz plane wave to the two-wire transmission line, there is an initial high loss corresponding to the coupled non-propagating modes and the propagating leaky modes. The leaky, radiating modes quickly disappear and the propagation becomes stable with a much smaller frequency dependent linear loss, from which we obtain the corresponding amplitude attenuation. It is important to note that for the 300 GHz simulation the initial coupling loss is the same for the Cu and PEC two-wire lines, but the stable PEC loss is much smaller (approaching zero) compared to the Cu line. The approach to zero is limited by the numerical accuracy of the simulation. The corresponding stable amplitude attenuation coefficients for the Cu line, indicated as the pink triangles in Fig. 9(b), are in good agreement with the analytic curve for the TEM mode.

Stated more precisely, the values of the simulated amplitude attenuation coefficients are 0.0018/cm at 50 GHz, 0.0040/cm at 100 GHz, 0.0050/cm at 200 GHz, 0.0065/cm at 300 GHz, and 0.0076/cm at 400 GHz. The corresponding power loss terms are 1.60 dB/m at 50 GHz, 3.47 dB/m at 100 GHz, 4.38 dB/m at 200 GHz, 5.62 dB/m at 300 GHz, and 6.56 dB/m at 400 GHz.

The stable propagating $\mathrm{E_y}$ vertical field pattern is shown in Fig. 12, and is also in good agreement with the TEM mode field pattern. Thus, we can conclude that to a good approximation the propagated pulses shown in Fig. 8 are propagating in the TEM mode of the two-wire transmission line, and that the extra loss shown by the Type-II two-wire line compared to the analytic TEM result is primarily due to the reduction of the conductivity in the skin depth.

The field pattern shown in Fig. 12, extends a distance of several times the wire separation, and is strongest in the plane of symmetry between the wires. Metallic and dielectric objects within the field pattern will cause reflections and coupling to the perturbation. Also, overlapping external signal fields will

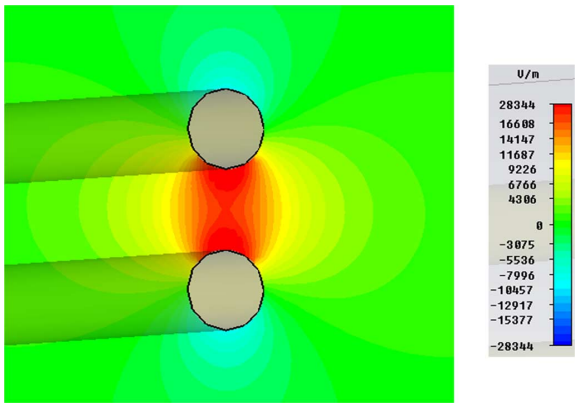

Fig. 12. Simulated 50 GHz propagating E_y (vertical) electric field pattern 42 mm down the line, which is in close agreement with the analytic TEM mode. The centers of the two wires are separated vertically by 1 mm.

couple unwanted cross-talk into the propagating wave. Therefore, for most applications it becomes important to shield the two-wire line.

We will now propose a possible embodiment for supporting and shielding the two-wire line. We have been able to construct two-wire lines with excellent mechanical precision by bonding to one surface of adhesive tape, usually 50 μm thick. However, the resulting THz performance has been limited by the attenuation of the tape and the adhesive. Our best results have been with 75 μm Teflon tape. The tape also has significant GVD due to the wavelength dependent fringing fields. The straight forward way to overcome these problems is to use a thin film tape of the order of 5 μm thick and made of material with low THz loss, similar in concept to the measurements on a co-planar transmission line on a thin dielectric layer [13]. Such a film holding the two-wires would be placed vertically with respect to Fig. 12.

For shielding the above two-wire line, consider the field pattern to be at the center of a cylindrical tube with a radius of 3 mm, three times the wire separation, and that the tube has been cut in half for the entire length. The adhesive side of the thin film tape can be attached to the outside edges of one of the half tubes, and the two wire line will be secured. Then the two half tubes can be taped together. The resulting tube, if metal provides shielding, or if plastic can be covered with metal foil or conducting tape. This simple example shows one promising approach to bring the two-wire line performance reported in this paper to the THz interconnect.

IV. Summary and Conclusions

In summary, we have demonstrated and characterized a chip to chip electrical interconnect that transmits 1.8 ps electrical pulses (extending over the frequency range from 50 to 300 GHz) with essentially no distortion a distance of 200 cm with a power loss of 5.8 dB/m. The observed pulses are capable of supporting a 100 Gb/s digital link, using this air spaced two-wire transmission line. Two tungsten probes efficiently couple the on-chip coplanar transmission line of the Tx to the two-wire line and from the two-wire line to the on-chip coplanar transmission line of the Rx. Because the two-wire line, the coplanar on-chip line and the dipole excitation switch have similar dipole field patterns, pulse generation, coupling and detection, are wide-band, non-dispersive and efficient.

The probes adiabatically transfer the propagating TEM mode of the coplanar line with 30 μm separation to the two-wire line with 1 mm separation between wires, thereby minimizing the excitation of higher order leaky-modes of the two-wire line. As confirmed by a numerical simulation, the air spaced two-wire lines show transform limited TEM mode pulse propagation with relatively low attenuation and very small GVD. The measured amplitude attenuation coefficient for the Type-II line is 1.31 times larger than theory for the TEM mode of the air-spaced two-wire Cu line, which can be explained primarily by the reduction of conductivity in the skin depth layer and some scattering by the variable wire separation.

If the practical problems of how to hold the two-wire lines, maintain the wire separation, and shield the wires, could be solved, this demonstrated capability would be sufficient to enable connection of such short pulses to the highest speed electronics and thereby provide some new science and technology opportunities.

Acknowledgment

The informative CST simulation was performed by G. J. Kim from Korea Electrotechnology Research Institute, Ansan, Korea. J. O'Hara provided several helpful readings of this manuscript.

References

[1] T.-I. Jeon and D. Grischkowsky, "Direct optoelectronic generation and detection of sub-ps-electrical pulses on sub-mm-coaxial transmission lines," *Appl. Phys. Lett.*, vol. 85, no. 25, pp. 6092–6094, 2004.

[2] J. W. Goodman, F. J. Leonberger, S. Y. Kung, and R. A. Athale, "Optical interconnections for VLSI systems," *Proc. IEEE*, vol. 72, no. 7, pp. 850–866, 1984.

[3] M. Forbes, J. Gourlay, and M. Desmulliez, "Optically interconnected electronic chips: A tutorial and review of the technology," *Electron. Commun. Eng. J.*, vol. 13, no. 5, pp. 221–232, 2001.

[4] H. Takahara, "Optoelectronic multichip module packaging technologies and optical input/output interface chip-level packages for the next generation of hardware systems," *IEEE J. Sel. Topics in Quantum Electron.*, vol. 9, no. 2, pp. 443–451, Mar./Apr. 2003.

[5] P. W. Coteus, J. U. Knickerbocker, D. H. Lam, and Y. A. Vlasov, "Technologies for exascale systems," *IBM J. Res. Develop.*, vol. 55, no. 5, pp. 14:1–14, 2011.

[6] M. B. Ketchen, D. Grischkowsky, T. C. Chen, C.-C. Chi, I. N. Duling, III, N. J. Halas, J.-M. Halbout, J. A. Kash, and G. P. Li, "Generation of sub-picosecond electrical pulses on coplanar transmission lines," *Appl. Phys. Lett.*, vol. 48, no. 12, pp. 751–753, 1986.

[7] M. van Exter and D. Grischkowsky, "Characterization of an optoelectronic terahz beam system," *IEEE Trans. Microw. Theory Techn.*, vol. 38, no. 11, pp. 1684–1691, 1990.

[8] D. Grischkowsky, "Optoelectronic characterization of transmission lines and waveguides by THz time-domain spectroscopy," *IEEE J. Sel. Topics in Quantum Electron.*, vol. 6, no. 6, pp. 1122–1135, Nov./Dec. 2000.

[9] R. W. McGowan, G. Gallot, and D. Grischkowsky, "Propagation of ultra-wideband short pulses of terahertz radiation through submillimeter-diameter circular waveguides," *Opt. Lett.*, vol. 24, no. 20, pp. 1431–1433, 1999.

[10] R. Mendis and D. Grischkowsky, "Undistorted guided-wave propagation of subpicosecond terahertz pulses," *Opt. Lett.*, vol. 26, no. 11, pp. 846–848, 2001.

[11] G. Goubau, "Open wire lines," *IRE Trans. Microw. Theory Techn.*, vol. MTT-4, no. 4, pp. 197–200, Oct. 1956.

[12] F. J. Lofy and T. K. Ishii, "Mode of millimeter wave two-wire surface wave transmission line fields," *Proc. IEEE*, vol. 53, no. 10, pp. 1652–1653, 1965.

[13] H.-J. Cheng, J. F. Whitaker, T. M. Weller, and L. P. B. Katehi, "Terahertz bandwidth characteristics of coplanar transmission lines on low permittivity substrates," *IEEE Trans. Microw. Theory Tech.*, vol. 42, no. 12, pp. 2399–2406, 1994.
[14] M. Mbonye, R. Mendis, and D. M. Mittleman, "A terahertz two-wire waveguide with low bending loss," *Appl. Phys. Lett.*, vol. 95, no. 23, p. 233506, 2009.
[15] H. Pahlevaninezhad, T. E. Darcie, and B. Heshmat, "Two-wire waveguide for terahertz," *Opt. Express*, vol. 18, no. 7, pp. 7415–7420, 2010.
[16] H. Pahlevaninezhad and T. E. Darcie, "Coupling of terahertz waves to a two-wire waveguide," *Opt. Express*, vol. 18, no. 22, pp. 22614–22624, 2010.
[17] P. Tannouri, M. Peccianti, P. L. Lavertu, F. Vidal, and R. Morandotti, "Quasi-TEM mode propagation in twin-wire THz waveguides," *Chinese Opt. Lett.*, vol. 9, no. 11, pp. 110013–110016, 2011.
[18] K. Wang and D. M. Mittleman, "Metal wires for terahertz wave guiding," *Nature*, vol. 432, pp. 376–379, 2004.
[19] T.-I. Jeon, J. Zhang, and D. Grischkowsky, "THz Sommerfeld wave propagation on a single metal wire," *Appl. Phys. Lett.*, vol. 86, no. 16, p. 161904, 2005.
[20] Y. B. Ji, E. S. Lee, J. S. Jang, S. H. Kim, and T.-I. Jeon, "Coupling properties of a conical tungsten-wire waveguide in the Terahertz frequency range," *J. Kor. Phys. Soc.*, vol. 53, no. 2, pp. 584–589, 2008.
[21] S. Ramo, J. R. Whinnery, and T. van Duzer, *Fields and Waves in Communication Electronics*, 3rd ed. New York, NY, USA: Wiley, 1993, p. 250.
[22] N. Laman and D. Grischkowsky, "Reduced conductivity in the Thz skin-depth layer of metals," *Appl. Phys. Lett.*, vol. 90, no. 12, p. 122115, 2007.
[23] A. J. Shutler and D. Grischkowsky, "Gap independent coupling into parallel plate THz waveguides using cylindrical horn antennas," *J. Appl. Phys.*, vol. 112, no. 7, p. 073102, 2012.
[24] T.-I. Jeon and D. Grischkowsky, "THz Zenneck surface wave (THz surface plasmon) propagation on a metal sheet," *Appl. Phys. Lett.*, vol. 88, no. 6, p. 061113, 2006.
[25] M. Gong, T.-I. Jeon, and D. Grischkowsky, "THz surface wave collapse on coated metal surfaces," *Opt. Express*, vol. 17, no. 19, pp. 17088–17101, 2009.
[26] N. Laman and D. Grischkowsky, "THz conductivity of thin metal films," *Appl. Phys Lett.*, vol. 93, no. 5, p. 051105, 2008.
[27] R. E. Collin, *Field Theory of Guided Waves*, 2nd ed. Piscacataway, NJ, USA: IEEE Press, 1990.
[28] Y. Leviatan and A. T. Adams, "The response of a two-wire transmission line to incident field and voltage excitation, including the effects of higher order modes," *IEEE Trans. Antennas Propag.*, vol. AP-30, no. 5, pp. 998–1003, May 1982.

Jeong Sang Jo received the B.S. and M.S. degrees in electrical and electronics engineering from the Korea Maritime University, Busan, south Korea, in 2011 and 2013, respectively.

Currently, he is with the Center for Quantum-Beam-based Radiation Research, Korea Atomic Energy Research Institute, Daejeon, Korea..

Tae-In Jeon received the B.S. and M.S. degrees in physics and electronics from Dong-A University, Busan Korea, in 1988 and 1990, respectively, and the Ph.D. degree in the School of Electrical and Computer Engineering, Oklahoma State University, Stillwater, OK, USA, in 1997 under the guidance of Prof. D. Grischkowsky. His Ph.D. dissertation was on the terahertz time-domain spectroscopy of semiconductors.

In 1998, he joined the Division of Electrical and Electronics Engineering, Korea Maritime University, Busan, Korea as an Assistant Professor and was subsequently promoted to Associate Professor and Full Professor. In the early years of his research, he focused on the characterization of the electrical and optical properties of carbon nanotubes and conducting polymers. After visiting professor at Oklahoma State University from 2004 to 2005, terahertz waveguides have been added to his interest.

Daniel R. Grischkowsky (SM'90-F'92) received the B.S. degree from Oregon State University, Corvallis, OR, in 1962, and the Ph.D. degree from Columbia University, New York, NY, in 1968.

In 1969, he joined the IBM Watson Research Center, Yorktown Heights, NY. In 1993, he joined Oklahoma State University, where his work has concentrated on unique applications of THz-TDS, including waveguides, the Sommerfeld wave, surface waves, hole arrays and photonic crystals.

Dr. Grischkowsky is a Fellow of the Optical Society of America (OSA) and the American Physical Society. He was awarded the 1985 Boris Pregel Award by the NY Academy of Sciences, the OSA 1989 R. W. Wood Prize, the OSA 2003 William F. Meggers Award, and the 2011 Kenneth J. Button Prize from the International Society of IR, MM and THz waves.